IRAQI JOURNAL OF APPLIED PHYSICS
Vol. 22, No. 2, April-June 2026, pp. 305-312

Fabrication and Comprehensive Characterization of Cr_2O_3-Doped Polypyrrole Thin Films for Enhanced Ethanol Gas Sensing Applications

Marwan Al-Lattouf
Muatazbullah I. Abdullah
Hiyam M. Ahmed*

[1] Physics Department, College of Education, Samarra University, Samarra, IRAQ
[2] Ministry of Education, Directorate General of Education in Kirkuk, Al-Jawhara Intermediate School for Girls, Kirkuk, IRAQ
[3] Department of Physics, College of Education for Women, Kirkuk University, Kirkuk, IRAQ
Corresponding author email: hiyammajeed@uokirkuk.edu.iq

Cr_2O_3-doped polypyrrole (PPy) thin films with 3.5, 5.5, and 7.5 wt.% loadings were fabricated on glass substrates using a simple drop-casting technique and comprehensively characterized. X-ray diffraction revealed improved crystallinity with doping, while clear surface evolution and larger effective surface area were revealed. Optical measurements indicated a progressive reduction of the bandgap from 2.83 eV (pure PPy) to 2.68 eV (7.5 wt.% Cr_2O_3), accompanied by enhanced electrical conductivity and carrier concentration confirmed by Hall and current–potential analyses. Gas-sensing tests toward ethanol at room temperature demonstrated markedly improved performance: the 7.5 wt.% Cr_2O_3 film achieving a maximum sensitivity of approximately 12% at 200 ppm with faster response and recovery than pristine PPy. These findings show that controlled Cr_2O_3 incorporation tailors the structural, electronic, and surface features of PPy, making the films strong candidates for low-cost, high-performance ethanol sensors operating under ambient conditions.

Keyword: PPy; Chromium oxide; Thin films; Drop casting; Hall effect; Gas sensors
Received: 18 August 2025; Revised: 9 October 2025; Accepted: 16 October 2025; Published: 1 April 2026

1. Introduction

Polypyrrole (PPy) is among the most prominent conductive polymers, attracting significant attention in recent decades due to its high electrical conductivity, excellent chemical stability, and ease of synthesis through cost-effective methods. PPy thin films have shown considerable potential in diverse applications, including flexible electronics, solar cells, and chemical sensors, particularly gas sensors, owing to their pronounced sensitivity to variations in the surrounding environment [1,2].

Doping PPy with metal oxides, such as chromium oxide (Cr_2O_3), has proven to be an effective approach for enhancing its physical and electrical properties. As a wide-bandgap semiconductor, Cr_2O_3 can improve charge transport, increase the effective surface area, and thereby enhance gas-sensing efficiency [3]. Among various transition metal oxides previously incorporated into PPy and other conducting polymers such as ZnO, TiO_2, and Fe_2O_3, Cr_2O_3 were specifically selected in this study because of its superior thermal and chemical stability, abundant surface oxygen vacancies, and high surface activity [4]. These features promote stronger interactions with ethanol molecules and facilitate charge transfer across the PPy matrix, leading to improved sensing response and selectivity. Additionally, Cr_2O_3 has been reported to maintain structural integrity under ambient conditions better than many other oxides, making it a promising dopant for stable, room-temperature ethanol sensors [5].

The drop-casting technique is one of the simplest and most widely employed methods for fabricating polymer thin films, offering straightforward control over film thickness and chemical composition, while enabling deposition on various substrates such as glass or silicon without compromising material purity [6,7].

Ethanol is a volatile organic compound (VOC) of considerable industrial and medical importance, widely utilized in industrial processes as a solvent and fuel. However, elevated concentrations of VOCs pose serious risks to human health and public safety. Consequently, the development of accurate and highly sensitive sensors capable of detecting ethanol at low operating temperatures, particularly at room temperature, has become an important research objective [8,9].

In the present work, thin films of pure PPy and PPy doped with Cr_2O_3 at different weight percentages (3.5%, 5.5%, and 7.5%) were fabricated on glass substrates via the drop-casting method. The structural

properties were characterized using X-ray diffraction (XRD), while surface morphology and topography were investigated using scanning electron microscopy (FESEM) and atomic force microscopy (AFM). Electrical properties were examined through Hall effect measurements, and electronic characteristics were evaluated via current–voltage (I–V) analysis. Furthermore, the gas-sensing performance toward ethanol at room temperature and at varying concentrations was assessed to determine the influence of Cr_2O_3 doping on sensor efficiency.

2. Experimental Part

2.1 Chemical Materials

Pure powdered polypyrrole (PPy) polymer (≥ 99%), nanoparticles of chromium oxide (Cr_2O_3, particle size <50nm, purity ≥99%), and dimethyl sulfoxide (DMSO, purity ≥99.9%) were used as a solvent. Polyvinylpyrrolidone (PVP, Mw ≈ 40,000) was added as a dispersing and stabilizing agent to prevent agglomeration of Cr_2O_3 nanoparticles and to promote uniform film morphology. During the subsequent annealing step at 120 °C, PVP is expected to partially decompose or volatilize and thus does not remain in significant amounts in the final film; therefore, it does not adversely affect the crystallinity or electrical conductivity of the PPy/Cr_2O_3 layers. All materials were used as received without further purification.

A total of 50 mg of PPy powder was dissolved in 10 mL of dimethyl sulfoxide (DMSO) to obtain a solution with a concentration of 5 mg/mL. The mixture was magnetically stirred at room temperature for 6 hours to achieve a homogeneous solution, followed by filtration through a PTFE membrane filter with a pore size of 0.45 μm to remove any undissolved particles.

Four different compositions were prepared as follows:

S1: Pure PPy (0 wt% Cr_2O_3)
S2: PPy + 3.5 wt% Cr_2O_3
S3: PPy + 5.5 wt% Cr_2O_3
S4: PPy + 7.5 wt% Cr_2O_3

The mass of Cr_2O_3 to be added was calculated by multiplying the PPy mass (50 mg) by the desired weight percentage. Accordingly, the added Cr_2O_3 masses were 1.75 mg, 2.75 mg, and 3.75 mg for S2, S3, and S4, respectively. The calculated amounts of Cr_2O_3 were dispersed in 5 mL of DMSO containing 0.5 wt.% PVP to achieve uniform nanoparticle dispersion and film homogeneity. The suspensions were ultrasonicated for 30 minutes, then added to the PPy solution and mechanically stirred for 15 minutes, followed by an additional 15 minutes of ultrasonication to ensure full homogenization.

Glass substrates (25×25 mm²) were cleaned by sequential immersion in acetone, ethanol, and distilled water, each for 10 minutes in an ultrasonic bath. After cleaning, the substrates were dried using a nitrogen jet under ambient laboratory conditions and then stored in a dust-free container until deposition. No additional surface energy modification was applied; however, the cleaning procedure provided sufficient wettability for uniform drop-casting.

Each glass substrate was placed horizontally inside a clean box. A specific volume of solution (approximately 200–300 μL) was placed in the center of the substrate using a micropipette, allowing the droplets to spread naturally over the surface. The films were initially dried on a hot plate at 80 °C for 30 minutes to evaporate the solvent. Gentle thermal annealing was then performed at 120 °C for 30 minutes under a continuous nitrogen flow (~100 sccm). Nitrogen was used to prevent oxidative degradation of PPy and Cr_2O_3 and to improve film stability, conductivity, and adhesion.

The structural, morphological, optical, electrical, and gas-sensing properties of the prepared thin films were comprehensively investigated. X-ray diffraction (PANalytical X'Pert PRO, Cu Kα, λ = 1.5406 Å, 40 kV, 30 mA) was performed over a 2θ range of 10°–80° to analyze the crystal structure. Surface morphology was examined using field-emission scanning electron microscopy (FE-SEM, FEI Nova Nano), while surface topography and RMS roughness were determined via atomic force microscopy (AFM, Bruker Dimension Icon) in tapping mode over a 5×5 μm² area. Optical properties were measured using a Shimadzu UV-2600 UV–Vis spectrophotometer (200-1100nm) to determine the optical band gap (E_g) via the Tauc method and assess absorption edge shifts induced by doping. Hall effect measurements (Ecopia HMS-5000, van der Pauw method, 0.55 T, room temperature) were conducted to evaluate charge carrier type, concentration, and mobility. Electrical behavior was studied through current–voltage (I–V) measurements using a Keithley 2400 Source/Measure Unit in the range of –5 V to +5 V under illumination. Gas-sensing performance toward ethanol (C_2H_5OH) was tested in a sealed chamber equipped with a temperature-controlled heater (25–200°C) and mass flow controller, with resistance changes monitored for concentrations of 50–500 ppm in dry air. Response and recovery times were recorded, and sensitivity was calculated using $S=Rg-Ra/Ra\times100$, where Ra and Rg represent the resistances in air and in the presence of ethanol gas, respectively [10].

3. Results and discussion

Figure (1) shows the XRD patterns of pure PPy and Cr_2O_3-doped PPy thin films. The diffraction profile of the undoped PPy film displays a broad halo centered at 2θ ≈ 22°, which is typical of predominantly amorphous PPy with only limited short-range ordering associated with the periodicity of the polymer backbone and weak π–π stacking between adjacent chains. The absence of sharp crystalline reflections confirms the lack of long-range order in pristine PPy [11].

Upon incorporation of Cr_2O_3 at concentrations of 3.5, 5.5, and 7.5 wt.%, a series of sharp and well-defined diffraction peaks appear at $2\theta \approx 20°$ (012), 24° (104), 33° (110), 36° (113), 41° (024), and 55° (116), corresponding to the hexagonal phase of Cr_2O_3 as indexed to JCPDS card 38-1479 [12]. The invariance of these peak positions with increasing dopant content indicates that Cr_2O_3 preserves its original crystal structure without undergoing phase transformations during film formation. Moreover, the progressive increase in the intensity and sharpness of the Cr_2O_3 peaks with higher doping levels suggests an enhancement in the overall degree of crystallinity and growth of Cr_2O_3 crystallites within the polymer matrix. Meanwhile, the broad PPy halo persists but with reduced relative intensity, signifying that the polymer matrix remains largely amorphous while the crystalline fraction of Cr_2O_3 becomes more dominant. This refined description clarifies that the films exhibit a composite structure an amorphous PPy background with dispersed and increasingly ordered Cr_2O_3 nanocrystals.

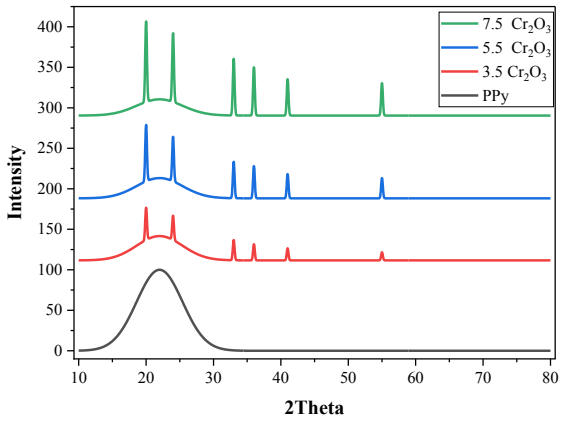

Fig. (1) XRD patterns of pure PPy films and doped with Cr_2O_3

The FE-SEM images in Fig. (2) show the progressive evolution of the surface morphology of pure PPy films and those doped with Cr_2O_3 at concentrations of 3.5%, 5.5%, and 7.5%. In the pure PPy film, the surface appears relatively homogeneous, consisting of small, tightly packed nanoclusters, with no evidence of sharp crystalline features consistent with the semi-amorphous nature of the polymer. Upon doping with 3.5% Cr_2O_3, the nanoparticles begin to aggregate into larger, more pronounced clusters, indicating the successful incorporation of Cr_2O_3 particles into the polymer matrix. Increasing the dopant concentration to 5.5% results in particles that are more distinct and exhibit a relatively narrow size distribution, along with improved surface regularity and enhanced nano-clustering features indicative of increased crystallinity and better structural cohesion.

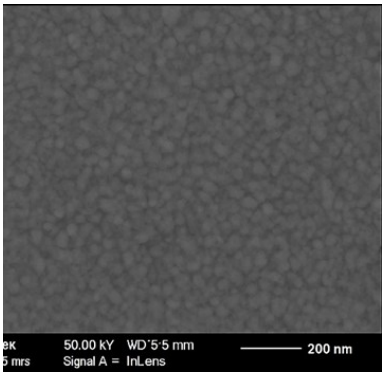

Pure PPy

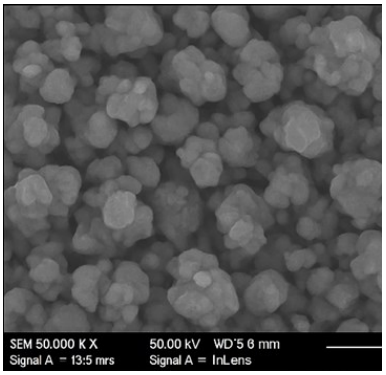

PPy + 3.5 wt.% Cr_2O_3

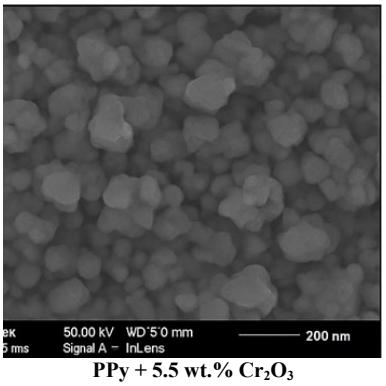

PPy + 5.5 wt.% Cr_2O_3

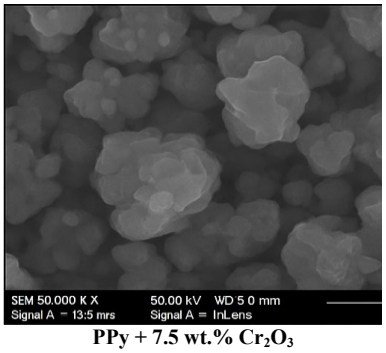

PPy + 7.5 wt.% Cr_2O_3

Fig. (2) FE-SEM images of pure and Cr_2O_3-doped PPy films

At the highest doping level of 7.5%, larger and more well-defined nanoparticles are observed, some with clear edges and signs of significant crystal growth, distributed relatively uniformly across the surface. This morphological progression demonstrates the role of

increasing Cr_2O_3 content in enhancing structural ordering, enlarging particle size, and improving crystalline characteristics, in agreement with the XRD results indicating a higher degree of crystallinity.

Figure (3) presents the AFM images showing the evolution of the surface topography of pure PPy films and those doped with Cr_2O_3 at concentrations of 3.5%, 5.5%, and 7.5%. The pristine PPy film exhibits a relatively smooth and quasi-homogeneous morphology with low-height nanoclusters and limited roughness. Upon doping with 3.5% Cr_2O_3, the height variation increases noticeably and dense, sharp protrusions emerge, suggesting the nucleation and localized growth of Cr_2O_3 nanoparticles and an increase in the effective surface area. At 5.5% Cr_2O_3, the number and prominence of protrusions decrease and the surface becomes more uniform with a narrower height distribution, indicating a more homogeneous dispersion of nanoparticles that suppresses large agglomerates and produces a compact, evenly distributed surface. When the doping level reaches 7.5%, however, excess Cr_2O_3 induces nanoparticle agglomeration and irregular cluster growth, creating pronounced height contrast between peaks and valleys and causing a marked increase in surface roughness. This non-monotonic roughness evolution indicates that moderate Cr_2O_3 content optimizes nanoparticle dispersion and smoothness, while excessive doping promotes aggregation and morphological irregularity. The quantitative roughness values (Ra and Rq) for all samples are summarized in table (1).

Table (1) Surface roughness parameters of pure and Cr_2O_3-doped PPy thin films

Sample	Cr_2O_3 content (wt.%)	Ra (nm)	Rq (nm)
S1	0	18 ± 2	23 ± 3
S2	3.5	38 ± 4	50 ± 5
S3	5.5	14 ± 2	19 ± 3
S4	7.5	45 ± 5	60 ± 6

Figure (4) shows the absorption spectra of pure PPy thin films and doped with Cr_2O_3 at concentrations of 3.5%, 5.5%, and 7.5% exhibit a distinct absorption peak in the 320-350nm range, attributed to π–π* transitions in the polyanion chains of PPy. In addition, a broad absorption band is observed in the visible to near-infrared region (600–900 nm), corresponding to polaron–π* and bipolaron–π* transitions associated with the conductive structure of PPy [13]. With the incorporation of Cr_2O_3, a gradual enhancement in absorption intensity is observed across the entire spectrum, most notably in the visible–near-infrared range, where the maximum absorbance is recorded at 7.5% Cr_2O_3. This enhancement is attributed to stronger interactions between the polymer matrix and Cr_2O_3 nanoparticles, which promote improved optical extension and broaden the absorption range [14]. The increased absorbance not only enhances the optical characteristics of the films but also positively influences their gas-sensing performance.

Higher light absorption facilitates the generation of a greater number of charge carriers and the activation of additional adsorption sites on the membrane surface, thereby improving surface interactions with target gas molecules. This, in turn, contributes to increased sensitivity and reduced response and recovery times. Consequently, adjusting the Cr_2O_3 doping level provides an effective approach for simultaneously enhancing the optical and electrical properties of the films, ultimately improving the operational efficiency of gas sensors.

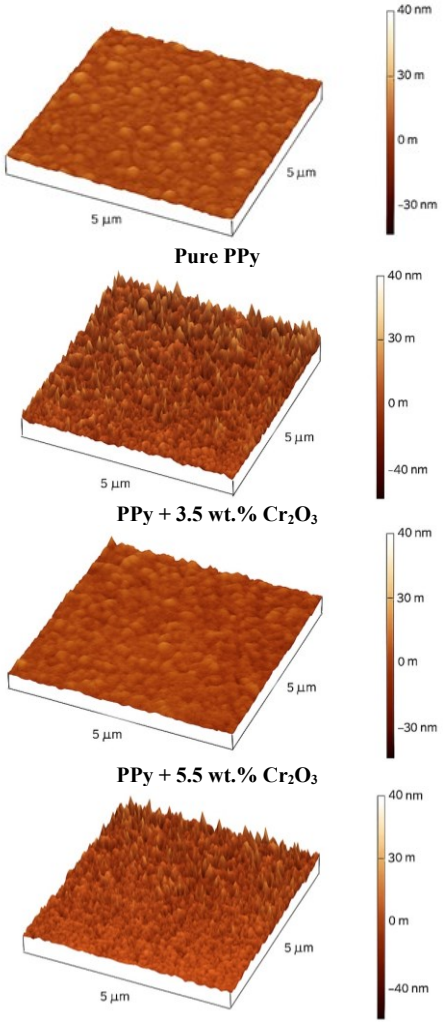

Fig. (3) AFM images of pure and Cr_2O_3-doped PPy films

Figure (5) shows Tauc's plots, of pure PPy thin films and doped with Cr_2O_3 at concentrations of 3.5%, 5.5%, and 7.5%. indicate the samples exhibit allowed direct electronic transitions. The results show that the energy band gap of pure PPy is approximately 2.83 eV, decreasing progressively with increasing Cr_2O_3 content to 2.78 eV (3.5% Cr_2O_3), 2.72 eV (5.5% Cr_2O_3), and 2.68 eV (7.5% Cr_2O_3). This reduction in energy

bandgap is attributed to the introduction of localized energy states within the polymer bandgap as a result of interactions between PPy chains and Cr_2O_3 nanoparticles [15]. These states facilitate electron transfer and extend the absorption edge toward longer wavelengths (redshift). Such modification of the films' electronic structure enhances electrical conductivity and increases surface activity, thereby improving their gas-sensing performance through more efficient adsorption/desorption processes and faster responses to target gas molecules.

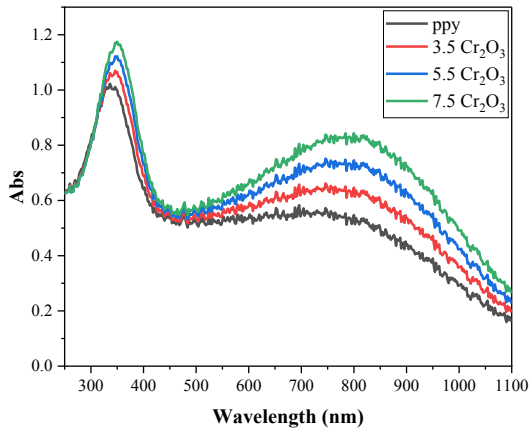

Fig. (4) Absorption spectra of pure and Cr_2O_3-doped PPy films

Hall effect measurements revealed that all films, both pure PPy and those doped with Cr_2O_3, exhibited p-type conductivity, as confirmed by the positive Hall coefficient and Hall voltage, indicating holes as the dominant charge carriers. The carrier concentration increased from 5.0×10^{17} cm^{-3} in the pure sample (S1) to 2.2×10^{18} cm^{-3} at a 7.5% Cr_2O_3 doping level (S4), as shown in table (1). This increase suggests that the incorporation of Cr_2O_3 introduces additional active conduction centers and facilitates charge transfer within the PPy matrix. Carrier mobility also improved from 0.35 to 0.50 $cm^2/V\cdot s$, resulting in enhanced electrical conductivity (from 0.028 to 0.1762 S/cm) and reduced resistivity (from 35.67 to 5.67 $\Omega\cdot cm$). These findings clearly confirm the p-type nature of the films and demonstrate that Cr_2O_3 doping effectively increases the density and mobility of majority carriers, which is beneficial for optimizing the electrical performance of PPy-based sensing devices [16].

Figure (6) shows the current–voltage (I–V) characteristics of pure PPy films and those doped with Cr_2O_3 at different concentrations (3.5%, 5.5%, and 7.5%). All samples exhibit clear Ohmic behavior, with the current increasing almost linearly as the applied voltage increases, indicating that conduction is primarily governed by charge transfer through good contact between the films and the electrodes. Doping PPy with Cr_2O_3 led to a pronounced increase in current at the same voltage, and this enhancement became more significant with higher doping levels, with the 7.5% Cr_2O_3 sample showing the highest current. This improvement in electrical conductivity is attributed to the increased free carrier concentration and enhanced charge mobility arising from the interaction between the polymer matrix and the Cr_2O_3 nanoparticles, in agreement with the Hall effect results. Such behavior reflects the improved electrical performance of the films, making them more effective for gas sensor applications, where higher conductivity enhances sensor response and sensitivity [17].

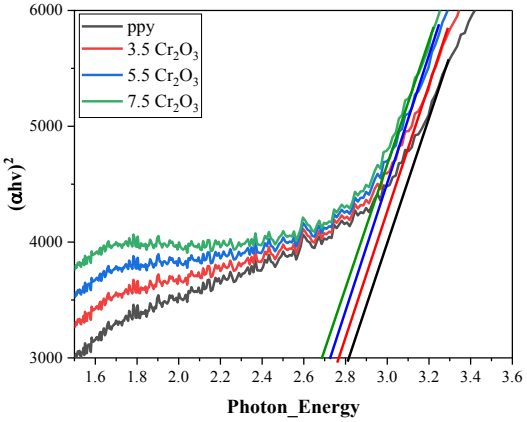

Fig. (5) Determination of energy bandgap of pure PPy films and Cr_2O_3-doped PPy films

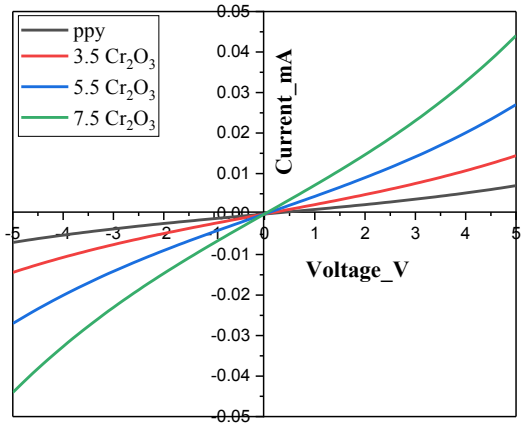

Fig. (6) Current-voltage characteristics of pure and Cr_2O_3-doped PPy films

Figure (7) shows the variation in resistance of pure PPy thin films and those doped with Cr_2O_3 at different ratios (3.5%, 5.5%, and 7.5%) as a function of ethanol gas concentration (10, 25, 50, 100, and 200 ppm) at room temperature. In all cases, the baseline resistance in air decreases as the Cr_2O_3 doping level increases; pure PPy exhibits the highest resistance, whereas the 7.5% Cr_2O_3-doped film shows the lowest. This reduction is associated with improved charge transport and the creation of additional conduction pathways due to the presence of Cr_2O_3 nanoparticles within the PPy matrix.

When exposed to ethanol, the resistance of the p-type PPy-based films increases with rising ethanol

concentration. Ethanol molecules act primarily as electron donors; their adsorption on the composite surface, especially at the abundant active sites and surface oxygen vacancies of Cr_2O_3, releases electrons that recombine with holes in the PPy matrix. This recombination reduces the hole density the majority carriers in PPy and thus increases the overall film resistance. The incorporation of Cr_2O_3 significantly enhances this sensing effect by providing more reactive sites and facilitating charge transfer at the PPy/Cr_2O_3 interface, which amplifies the resistance change and improves ethanol detection sensitivity under ambient conditions [18].

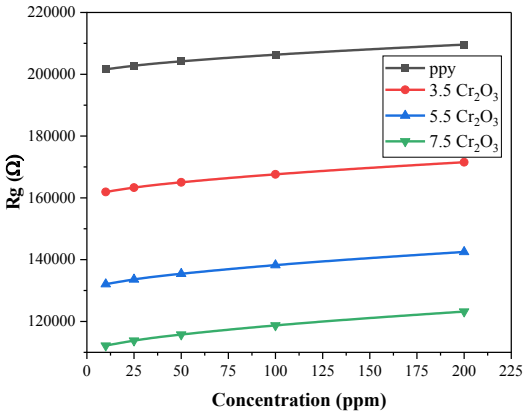

Fig. (7) Variation of resistance with gas concentration for pure and Cr_2O_3-doped PPy films

Figure (8) shows the variation in sensitivity (%) of pure PPy) films and doped with Cr_2O_3 at different concentrations (3.5%, 5.5%, and 7.5%) as a function of ethanol gas concentration (10, 25, 50, 100, 200 ppm) at room temperature. The results show a clear and significant increase in sensitivity with rising gas concentration for all samples, which is attributed to the larger number of ethanol molecules adsorbed on the active surfaces of the films, leading to more pronounced changes in their electrical properties.

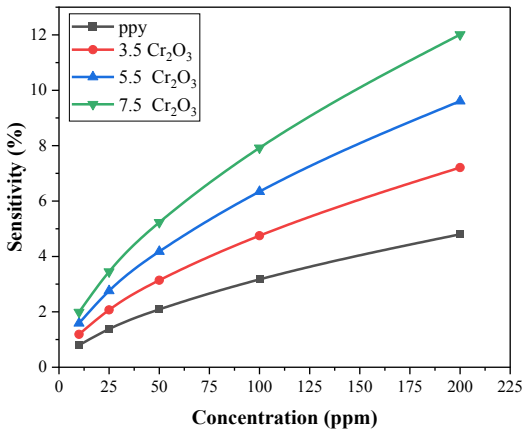

Fig. (8) Variation of sensitivity with gas concentration for pure and Cr_2O_3-doped PPy films

Doping with Cr_2O_3 markedly enhanced the sensitivity compared to pure PPy, with the 7.5% Cr_2O_3-doped sample achieving the highest sensitivity (~12%) at 200 ppm, while the pure PPy sample exhibited the lowest value (~4.9%). This enhancement is explained by the role of Cr_2O_3 nanoparticles in increasing the effective surface area and the number of active sites available for gas interaction, as well as improving charge transport within the hybrid structure [19]. These findings indicate that increasing the doping ratio enhances the sensor's efficiency in detecting ethanol at low concentrations and at room temperature, making it a promising candidate for practical applications in air quality monitoring and flammable gas detection.

Figures (9) show the response and recovery times of pure PPy films and doped with Cr_2O_3 when exposed to ethanol gas at various concentrations (10, 25, 50, 100, 200 ppm) at room temperature. The results clearly show that the response time decreases markedly with increasing gas concentration. Pure PPy exhibited the longest response time, approximately 60 s at the lowest concentration, whereas this time gradually decreased with higher doping levels, reaching about 19 s at 200 ppm for the PPy+7.5% Cr_2O_3 samples. This improvement is attributed to the increased number of active sites introduced by the Cr_2O_3 nanoparticles, which facilitate gas molecule adsorption and accelerate the generation of the electrical signal [20]. In contrast, the recovery time displayed an inverse trend generally increasing with gas concentration but significantly decreasing with higher doping ratios.

Pure PPy recorded the longest recovery time, exceeding 130 s at the highest concentration, while the 7.5% Cr_2O_3-doped samples recovered in approximately 95 s. This reduction indicates that the incorporation of Cr_2O_3 enhances desorption process by improving film porosity and electrical conductivity, thereby enabling faster restoration of the membrane's baseline electrical properties. Such behavior underscores the potential of Cr_2O_3-doped PPy films for practical sensing applications that demand short response and recovery times.

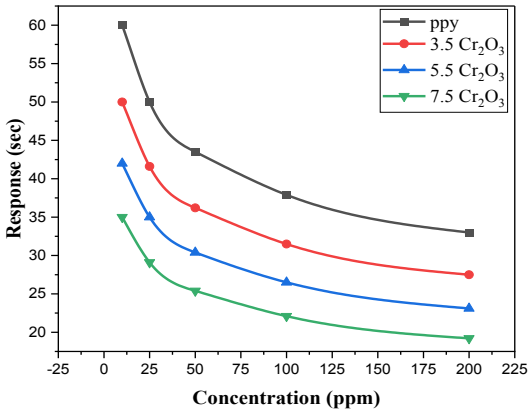

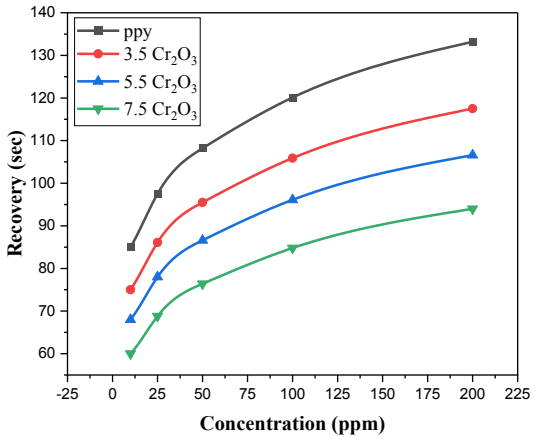

Fig. (9) Response and recovery times for pure and Cr_2O_3-doped PPy films

Figure (10) shows the dynamic properties of gas sensors fabricated from pure PPy and PPy doped with varying concentrations of Cr_2O_3 (3.5%, 5.5%, and 7.5%). The response and recovery times were evaluated upon exposure to ethanol gas at a concentration of 100 ppm under fixed operating conditions (t_{on} = 60 s, t_{off} = 60 s, 7 ON pulses, and a recording interval of 0.5 s).

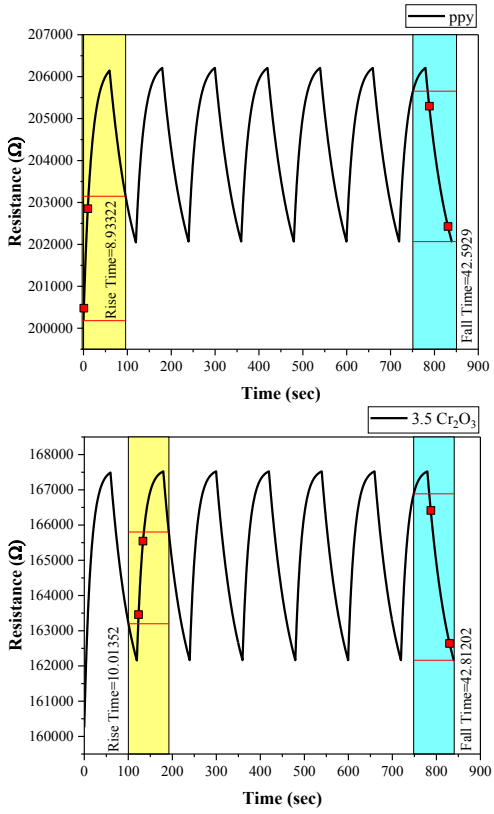

The results revealed that the response time ranged from 8.93 s for pure PPy to 11.61 s for the 5.5% Cr_2O_3-doped sample, while the recovery time varied from 42.59 s to 32.39 s, respectively. These findings indicate that the adsorption process on the sensor surface occurs relatively quickly, whereas recovery is slower due to the gradual desorption of ethanol molecules. This behavior is consistent with that typically observed in conductive polymer-based sensors supported by metal oxides. Moreover, Cr_2O_3 doping was found to influence both response and recovery times by increasing the density of active sites and enhancing surface conductivity. This agrees with the findings of [21], which reported that incorporating nanoscale metal oxides into conductive polymers improves the dynamic sensing response through enhanced electron transport and increased surface interaction with target gas molecules.

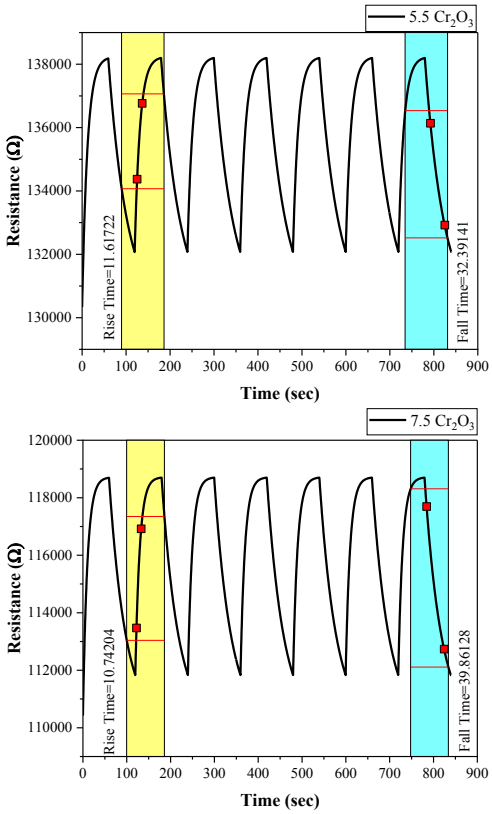

Fig. (10) Analysis of dynamic properties of pure and Cr_2O_3-doped PPy films

4. Conclusion

This study demonstrates that doping polypyrrole (PPy) thin films with chromium oxide (Cr_2O_3) using a simple, low-cost drop-casting method significantly enhances their structural, electrical, and ethanol gas-sensing properties at room temperature. Cr_2O_3 incorporation improves crystallinity, tunes surface roughness, increases effective surface area, and narrows the optical band gap, resulting in higher carrier concentration and conductivity. These synergistic modifications lead to superior ethanol detection, with the 7.5 wt.% Cr_2O_3 film achieving the highest sensitivity and faster response and recovery compared to undoped PPy. The results establish a clear structure–property relationship and highlight the potential of Cr_2O_3-doped PPy films for practical, ambient ethanol sensing.

References

[1] M.I. Abdullah, A.R. Ahmad and A.F. Abdulameer, "Polypyrrole thin films decorated with gold and silver nanoparticles for humidity sensor application", *AIP Conf. Proc.*, 2977(1) (2023).

[2] J. Lou et al., "Preparation and Electrochromic Properties of MnO_2/PPy Composite Films with Coral-like Structures", *ACS Appl. Mater. Interfaces*, 16(28) (2024) 36942-36952.

[3] A.V. Almaev et al., "Structural, electrical and gas-sensitive properties of Cr_2O_3 thin films", *Superlatt. Microstruct.*, 151 (2021) 106835.

[4] N.V. Iyer et al., "Contemporary advances in metal oxide doped polypyrrole composites: a comprehensive review", *Int. J. Nanosci. Nanotech.,* 20(2) (2024) 143-159.

[5] N. Dhariwal et al., "Ethanol sensing materials and device using Co^{2+}, Zn^{2+}, Cr^{2+} doped α-Fe_2O_3 nano-particles with room temperature response/recovery", *Sens. Actuat. B: Chem.,* 390 (2023) 134037.

[6] M. Libber, N. Gariya and M. Kumar, "A comprehensive analysis of supercapacitors with current limitations and emerging trends in research", *J. Solid State Electrochem.*, 29(2) (2025) 513-527.

[7] K. Khaldi et al., "Chemical synthesis of quaternary hybrid conducting polymers@Cr_2O_3-graphene oxide electrodes with excellent performance in supercapacitors", *J. Inorg. Organomet. Polym. Mater.,* 35(1) (2025) 58-71.

[8] L.L. Cardoso et al., "Chemical composition and production of ethanol and other volatile organic compounds in sugarcane silage treated with chemical and microbial additives", *Animal Prod. Sci.,* 59(4) (2018) 721-728.

[9] S. Qureshi et al., "Fractional modeling of blood ethanol concentration system with real data application", *Chaos: An Interdiscip. J. Nonl. Sci.,* 29(1) (2019) 013143.

[10] J. Janata, "**Principles of Chemical Sensors**", Springer Science & Business Media (2009).

[11] A.-U.D. Sabah, I.M. Ibrahim and M.G. Hammed, "Electrochemical supercapacitors of PPy/GO-CoO prepared by hydrothermal method for energy storage", *Ionics,* 31 (2025) 9815-9828.

[12] H.M. Kamari et al., "Comprehensive study on morphological, structural and optical properties of Cr_2O_3 nanoparticle and its antibacterial activities", *J. Mater. Sci.: Mater. Electron.,* 30(8) (2019) 8035-8046.

[13] N. Luhakhra and S.K. Tiwari, "Polaron and bipolaron mediated photocatalytic activity of polypyrrole nanoparticles under visible light", *Colloids Surf. A: Physicochem. Eng. Asp.,* 667 (2023) 131380.

[14] H.K. Inamdar et al., "Polypyrrole/Cr_2O_3 hybrid nanocomposites (NCs) prepared for their structural, morphological, optical and conductivity studies", *Compos. Commun.,* 14 (2019) 21-28.

[15] M. Rabia, E. Aldosari and A.H.A. Geneidy, "Exceptionally crystalline nature of CrO_3-Cr_2O_3/Ppy nanocomposite as a prospective photoelectrode for efficient green hydrogen generation in the context of environmentally friendly water-splitting reactions using sanitized water", *Environ. Prog. Sustain. Ener.,* 43(5) (2024) e14455.

[16] F.J. Hameed et al., "Enhancing optical and electrical gas sensing properties of polypyrrole nanoplate by dispersing nano-sized tungsten oxide", *ECS J. Solid State Sci. Technol.,* 10(10) (2021) 107001.

[17] A. Joseph et al., "Amorphous Cr_2O_3 sheets: a novel supercapacitor electrode material", *ChemistrySelect,* 7(40) (2022) e202203049.

[18] S. Tang et al., "Construction of mesoporous Fe_2O_3/Cr_2O_3 np heterojunctions for efficient improvement of low-concentration acetone detection and gas-sensing mechanism", *Rare Metals*, 44 (2025) 4851-4867.

[19] S. Lee et al., "Chemoresistive Gas Sensors for Food Quality Monitoring", *J. Semicond. Technol. Sci.,* 22(4) (2022) 244-258.

[20] M. Rabia et al., "Porous-spherical Cr_2O_3-Cr(OH) 3-polypyrrole/polypyrrole nanocomposite thin-film photodetector and solar cell applications", *Coatings*, 13(7) (2023) 1240.

[21] S.M. Yenorkar et al., "Polymer- Metal Oxide Composite (PPy–MoO_3) for Ammonia and Ethanol Gas Sensor", *Macromol. Symposia,* 400(1) (2021) 2100049.

Table (2) Hall effect parameters of pure PPy and Cr_2O_3-doped PPy thin films

Sample	Carrier Type	Carrier Concentration (cm^{-3})	Mobility ($cm^2/V{\cdot}s$)	Conductivity (S/cm)	Resistivity (Ω·cm)	Hall Coefficient (cm^3/C)	Hall Voltage (V)
(PPy)	p-type	5.0×10^{17}	0.35	0.0280	35.6697	12.4844	1716.60
(PPy+3.5wt%Cr_2O_3)	p-type	9.0×10^{17}	0.40	0.0577	17.3394	6.9358	953.67
(PPy+5.5wt%Cr_2O_3)	p-type	1.5×10^{18}	0.45	0.1081	9.2477	4.1615	572.20
(PPy+7.5wt%Cr_2O_3)	p-type	2.2×10^{18}	0.50	0.1762	5.6747	2.8374	390.14

